ARTICLE

Age-dependent alterations in key components of the nigrostriatal dopaminergic system and distinct motor phenotypes

Jiang-peng Fan[1], Hui-zhen Geng[2,3], Ya-wei Ji[2,3], Tao Jia[2,3], Jennifer B. Treweek[4], An-an Li[1], Chun-yi Zhou[2,3,4], Viviana Gradinaru[4] and Cheng Xiao[2,3,4]

The nigrostriatal dopaminergic (DA) system, which includes DA neurons in the ventral and dorsal tiers of the substantia nigra pars compacta (vSNc, dSNc) and DA terminals in the dorsal striatum, is critically implicated in motor control. Accumulating studies demonstrate that both the nigrostriatal DA system and motor function are impaired in aged subjects. However, it is unknown whether dSNc and vSNc DA neurons and striatal DA terminals age in similar patterns, and whether these changes parallel motor deficits. To address this, we performed ex vivo patch-clamp recordings in dSNc and vSNc DA neurons, measured striatal dopamine release, and analyzed motor behaviors in rodents. Spontaneous firing in dSNc and vSNc DA neurons and depolarization-evoked firing in dSNc DA neurons showed inverse V-shaped changes with age. But depolarization-evoked firing in vSNc DA neurons increased with age. In the dorsal striatum, dopamine release declined with age. In locomotor tests, 12-month-old rodents showed hyperactive exploration, relative to 6- and 24-month-old rodents. Additionally, aged rodents showed significant deficits in coordination. Elevating dopamine levels with a dopamine transporter inhibitor improved both locomotion and coordination. Therefore, key components in the nigrostriatal DA system exhibit distinct aging patterns and may contribute to age-related alterations in locomotion and coordination.

Keywords: aging; substantia nigra pars compacta; dopaminergic neurons; dopamine sensor; locomotion; coordination; rodent

Acta Pharmacologica Sinica (2022) 43:862–875; https://doi.org/10.1038/s41401-021-00713-5

INTRODUCTION

Motor decline is among the most visible symptoms of old age, and its common manifestations include deficits in reaction time, coordination skills, and the speed and accuracy of motor responses [1–5]. Although muscle atrophy and imbalanced energy homeostasis contribute significantly to motor decline in aged subjects [6–8], the role of structural and biochemical alterations in the central nervous system, especially in brain regions involved in motor control, cannot be neglected [5, 9–12]. Specifically, the nigrostriatal dopaminergic (DA) system, consisting of DA neurons in the substantia nigra pars compacta (SNc) and DA terminals in the dorsal striatum, is compromised during aging, with degeneration of SNc DA neurons [4, 13, 14] and reduction of dopamine release in the striatum [4, 10]. Furthermore, motor dysfunction in the elderly can be temporarily rescued with dopamine compensation treatment [9, 12, 15]. These lines of evidence hint that impairment of the nigrostriatal DA system may be associated with motor deficits in aging. However, this association awaits further confirmation, such as elaboration of the correlation between dysfunction in the key components of the nigrostriatal DA system and distinct motor phenotypes.

Previous pioneering anatomical studies delineated SNc DA neurons into dorsal and ventral tiers (dSNc and vSNc) [16, 17]. Both tiers are implicated in motor control [18–21]. Morphological studies have demonstrated that vSNc DA neurons are more vulnerable to aging than dSNc DA neurons [4, 22]. However, electrophysiological studies have not reached a consensus about age-related alterations in the activity of dSNc DA neurons [23–25]. Until now, no study has elucidated age-dependent changes in the activity of vSNc DA neurons. Besides dSNc and vSNc DA neurons, DA terminals in the dorsal striatum release less dopamine in aged subjects [4, 10, 26]. However, it is unclear whether dSNc and vSNc DA neurons and striatal DA terminals are similarly or differentially modified in the aging process.

Locomotion and coordination are essential motor behaviors across species, and can be reliably assessed with open field, beam walking, and rotarod tests in rodents [27, 28]. Several studies demonstrated that physical inactivity and the impaired coordination skills commonly seen in the elderly [5, 29] may be associated with dysfunction of the nigrostriatal DA system. For instance, degeneration or inhibition of dSNc DA neurons underlies difficulties in movement initiation and movement slowness [18–

[1]Jiangsu Province Key Laboratory in Brain diseases, Department of Biochemistry and Molecular Biology, School of Basic Medicine, Xuzhou Medical University, Xuzhou 221004, China; [2]Jiangsu Province Key Laboratory in Anesthesiology, School of Anesthesiology, Xuzhou Medical University, Xuzhou 221004, China; [3]NMPA Key Laboratory for Research and Evaluation of Narcotic and Psychotropic Drugs, School of Anesthesiology, Xuzhou Medical University, Xuzhou 221004, China and [4]Division of Biology and Biological Engineering, California Institute of Technology, Pasadena, CA 91125, USA
Correspondence: Chun-yi Zhou (chunyi.zhou@xzhmu.edu.cn) or Cheng Xiao (xchengxj@xzhmu.edu.cn)

Aging nigrostriatal dopaminergic system and motor deficits
JP Fan et al.

863

[20], whereas stimulation of dSNc DA neurons facilitates locomotion and determines the vigor of future movements [19, 20]. Pharmacological enhancement of the nigrostriatal DA system improves coordination skills in aged mice [9, 15]. We hypothesize that, during the process of aging, distinct motor deficits in locomotion and coordination develop in concordance with dysfunction of particular components of the nigrostriatal DA system.

In this study, we performed electrophysiological recordings from dSNc and vSNc DA neurons in rats, measured dopamine release in the dorsal striatum with a dopamine sensor [30] in mice, and analyzed motor behaviors in aging cohorts of rats and mice (6, 12, 18, and 24 months old). We found similar age-dependent alterations between the excitability of SNc DA neurons and exploratory behavior, and between striatal dopamine release and coordination. Additionally, pharmacological elevation of dopamine improved both locomotion and coordination in aging mice. Therefore, components of the nigrostriatal DA system may be potential targets for the alleviation or delay of age-related motor phenotypes.

MATERIALS AND METHODS
Animals
We used wild-type male Long-Evans rats from Charles River Laboratory (South San Francisco, CA, USA) and C57BL6 mice from Jinan Pengyue Laboratory Animal Breeding Co. Ltd. (Jinan, Shandong, China). Animal husbandry and all experimental procedures for the use of rats and mice were approved by the Institutional Animal Care and Use Committee (IACUC) and by the Office of Laboratory Animal Resources at the California Institute of Technology and at the Xuzhou Medical University, following the NIH Guide for the Care and Use of Laboratory Animals. Male rats were double-housed with ad libitum access to food and water, and subjects were recruited into our study cohorts at 5 months of age. Thereafter, the rats were single-housed because of body size in an environment with a 12-h light/dark cycle and stable temperature (22–24.5 °C) and humidity (40%–60%). Male mice were group-housed (≤4 per cage) on a 12-h light/dark cycle, with free access to water and food. The mice were randomly allocated into different age groups and were subjected to experiments when they met the age criterion. Efforts were made to minimize animal suffering and to reduce the number of animals used.

Patch-clamp recordings of SNc neurons in brain slices
In this study, we used 6-, 12-, and 24-month-old wild-type Long-Evans rats to characterize the electrophysiological properties of SNc DA neurons. To improve the cell viability of acutely prepared midbrain slices, we sectioned rat brains parasagittally to mitigate the detrimental effects of severing long-range projections on the survival of DA neurons, and modified the protocol we described previously [21, 31–33]. For detection of dopamine release, we prepared coronal brain slices from mice. In brief, rats and mice were euthanized with carbon dioxide, and subjected to cardiac perfusion with ice-cold modified sucrose-based artificial cerebral spinal fluid (SACSF) saturated with 95% O_2/5% CO_2 (carbogen) containing (mM): 85 NaCl, 2.5 KCl, 1.2 NaH_2PO_4, 4 $MgCl_2$, 0.5 $CaCl_2$, 24 $NaHCO_3$, 25 glucose, and 70 sucrose. The brain was subsequently removed and slowly (advance speed of 0.04 mm/s) sliced with a vibratome (VT-1200, Leica Inc.) while immersed in ice-cold SACSF. Brain slices (300 μm) containing the substantia nigra or the striatum were then allowed to recover at 32 °C in a holding chamber filled with carbogenated SACSF. Seventy-five minutes later, SACSF in the holding chamber was replaced with regular ACSF (32 °C, carbogenated), containing (mM): 125 NaCl, 2.5 KCl, 1.2 NaH_2PO_4, 1.2 $MgCl_2$, 2.4 $CaCl_2$, 26 $NaHCO_3$, and 11 glucose. The chamber with brain slices was placed at room temperature for at least half an hour before the slices were transferred for patch-clamp recordings and live imaging.

Slices were transferred to the recording chamber of the patch-clamp rig, and carbogen-saturated ACSF at 32 ± 0.5 °C was constantly perfused at a flow rate of 1.5–2.0 mL/min. The dSNc and vSNc in parasagittal brain slices were identified according to the rat brain atlas by viewing the slices through a 4× objective under near-infrared DIC illumination with an upright microscope (BX50WI, Olympus; or FN-1, Nikon) equipped with a CMOS CCD camera (Flash 4.0, Hamamatsu). The neurons were visualized through a 40× water-immersion objective (NIR APO, NA: 0.80, WD: 3.5 mm). Whole-cell patch-clamp techniques were used to record electrophysiological signals with a MultiClamp 700B amplifier (Molecular Devices), a Digidata 1440 A or 1552B analog-to-digital converter (Molecular Devices), and pClamp 10.4 software (Molecular Devices). Data were sampled at 10 kHz and filtered at 2 kHz. Patch electrodes had a resistance of 4–6 MΩ when filled with the intrapipette solution (mM): 135 K gluconate, 5 KCl, 0.2 EGTA, 0.5 $CaCl_2$, 10 HEPES, 2 Mg-ATP, 0.1 GTP, and 0.2% neurobiotin (for subsequent identification of neuronal type). The pH of the solution was adjusted to 7.2 with Tris-base and the osmolarity was adjusted to 300 mOsm with sucrose. The junction potential between the patch pipette and the bath solution was nulled just before gigaseal formation. Series resistance was monitored without compensation throughout the experiment. Data were discarded if the series resistance (11–20 MΩ) changed by more than 20% during whole-cell recordings. We recorded and labeled one neuron in each slice and used 6–8 slices from each animal.

Electrophysiological data were analyzed with Clampfit 10.4 (Molecular Devices). We used the "event detection feature" to analyze action potentials, including the frequency and the coefficient of variation of the frequency. The firing pattern was classified as irregular if the neurons fired with alternately faster and slower firing rates [34]; otherwise, the firing pattern was classified as regular. Current steps (2 s) from 0 to 260 pA with a 20 pA increment were injected sequentially into current-clamped neurons to evoke repetitive firing. These data were used to depict the stimulus–response relationship.

Identification of neuron type with neurobiotin and immunohistochemistry
After whole-cell patch-clamp recordings, the brain slices were transferred into 4% paraformaldehyde (PFA) in PBS in a 24-well plate, taking care to ensure that the side with the recorded neurons faced up. Slices were fixed for 45–60 min, followed by three washes with PBS (10 min each). The slices were then immunostained according to the following procedure. The slices were permeabilized for 1 h in PBS/0.1% Triton-X 100, blocked for 1 h in PBS/10% donkey serum, incubated in chicken anti-TH antibody (1:1000, Aves labs) and Alexa 555-conjugated streptavidin (1:500, Life Technology) in PBS/4% donkey serum at 4 °C for 18 h, washed three times (15 min each) in PBS, incubated in Alexa 488-conjugated secondary antibodies (goat anti-chicken antibody, 1:500, Jackson ImmunoResearch Lab) in PBS/4% donkey serum at room temperature for 1.5 h. Samples were washed three times (10 min each) in PBS, dried at room temperature, immersed in mounting medium (Vector laboratories Inc.), and cover-slipped.

Low and high magnification images were acquired with a Zeiss LSM 780 or LSM 880 confocal microscope, controlled by Zen 2011 or Zen2 acquisition software (Zeiss). The images were processed with Image J [35].

Determination of dopamine release
We employed a viral vector-assisted method to transfect a dopamine sensor (AAV-hSyn-GRAB-DA3.3), developed by Sun et al [30]., in the dorsal striatum in mice. After 3 weeks' recovery, the mice were sacrificed and live striatal slices were prepared. The slices were transferred into an imaging chamber on the specimen

864

stage of an upright epi-fluorescent microscope (FN-1, Nikon, Japan), and were perfused with carbogenated ACSF. A field in the dorsal striatum expressing GRAB-DA was brought into focus, and a sequence of fluorescence images under eGFP illumination (15 frames/s) were acquired with HCImage 4.1 software (Hamamatsu, Japan) through a CCD-Camera (Hamamatsu, Flash 4.0 LTE) to monitor the fluorescence intensity of GRAB-DA. An electrode was placed in the matrix of the dorsal striatum to deliver electrical stimulation (100 μs, 25 μA), as described in the Results section. The mean intensity of fluorescence around the stimulation electrode was measured with HCImage 4.1 and the time course was plotted with SigmaPlot 14.0.

Behavioral assays
The male rats were singly housed in a rat behavior testing room. The group-housed mice were moved into a mouse behavior testing room and habituated at least for 1 h before tests. Before the start of each behavioral test, subjects were handled or trained for 3 days (10 min per day) and were granted 10 min free exploration with each behavioral apparatus. The behavioral apparatus was sanitized between subjects with Accel surface disinfectant cleaner (Research Supply Company) or 75% alcohol. All behavioral assays for rats were conducted during subjects' dark cycle. All assays for mice were carried out during their light cycle.

Open field test. A rat was placed in a square open field arena (50 cm × 50 cm). A mouse was placed in a round open field arena (30 cm in diameter). They were allowed to move freely within the arena for 30 min [21, 28, 33]. During this period, locomotor activity was acquired with a video camera controlled by Ethovision software (XT 9 or XT 14, Noldus Information Technology) [21, 33, 36]. The data were analyzed off-line, and the Ethovision subject-tracking capability was used to quantify travel distance, mobility, and moving velocity (distance/mobility time) in animals.

Balancing beam. The apparatus was a 3-cm wide and 40-cm long beam, which was lifted 80 cm above the floor [37]. Rats were trained to balance on the beam four–five times each day for 3 days before testing. During the test session, we recorded how long the subjects spent on the beam before falling off, with a cut-off time of 6 min.

Cylinder test. Testing was performed in cylinders that measured 50 cm in height and 15 cm in diameter [38]. Each subject was placed in the cylinder and allowed to freely explore for 10 min while movements were recorded with a video camera. The time spent in rearing was analyzed off-line.

Beam walking. A 100-cm long round beam (1.5 cm in diameter) was lifted 60 cm above the floor [27]. Mice were trained to walk across the beam four–five times each day for 3 consecutive days before testing. During the test session, we recorded the latency for the mice to traverse the beam and number of slips the mice experienced during the crossing.

Rotarod. The rotarod assay was performed according to a previously reported method [27]. After habituation to the testing room, mice were placed on a rotarod (SANS-SA102, China) for training (three times per day for 3 consecutive days with an interval of at least 15 min between sessions on the same day). The rotating rod (3 cm in diameter) had 1 mm grips, and was positioned 16 cm above the instrument floor. The rotation speed of the rod was initially set to 5 rotations per min (rpm), and gradually increased by 7 rpm up to 40 rpm. The apparatus had six lanes separated with flanges and allowed six mice to be tested at the same time. The latency and rotation speed when the mice fell off the rod were recorded.

Data analysis
Statistical analyses were performed in SigmaPlot 14.0 (SPSS Inc.) and OpenEpi Version 2.3.1 (an online tool) [39]. Summary data were presented as scatter plots and bar charts. Multiple-group data were compared with one-way or two-way ANOVA (if the data passed tests of both normality and equal variance) or Kruskal–Wallis one-way ANOVA on ranks (if the data failed either or both tests). If statistical significance was found among three or more groups, a pairwise comparison was performed, as specified in the figure legend. The incidence of an event among groups was compared with 2 × 2 or 2 × 3 chi-square tests. For statistics, two-tailed P values were generated with Sigmaplot or OpenEpi and $P < 0.05$ was considered statistically significant.

RESULTS
Electrophysiological properties of adult dSNc and vSNc DA neurons
Using immunostaining of tyrosine hydroxylase (TH) in rat midbrain slices, we observed DA neurons not only in the dorsal tier of the SNc (dSNc), but also in the caudal part of the ventrolateral substantia nigra (Fig. 1a). These neurons formed an island amidst the ventral part of the substantia nigra pars reticulata. This phenomenon was reported in previous pioneering anatomical studies [16, 17], which refer to the island as the ventral tier of the SNc (vSNc). The electrophysiological properties of dSNc DA neurons and age-dependent alterations in these neurons have been characterized in numerous studies [24, 25, 40–43] but such information remains absent for vSNc DA neurons. To fill this gap, we performed patch-clamp recordings of both dSNc and vSNc neurons in ex vivo brain slices from rats. The recorded neurons were labeled with 0.2% neurobiotin and were identified as DA neurons with post hoc TH-staining (Fig. 1b).

To address whether baseline activity differs between dSNc and vSNc DA neurons, we performed cell-attached patch-clamp recordings of dSNc and vSNc neurons in brain slices from young adult (6-month-old) rats. We observed spontaneous firing in 74% (23/31) of dSNc DA neurons and 91% (10/11) of vSNc DA neurons ($x^2 = 1.35$, $P = 0.25$). Among neurons showing spontaneous firing, about 40%−50% of them exhibited an irregular firing pattern (Fig. 1c, d). Although the spontaneous firing rate was similar between dSNc DA neurons with regular (dSNc-R) and irregular (dSNc-I) firing patterns, it was significantly higher in vSNc DA neurons with regular firing (vSNc-R) than those with irregular firing (vSNc-I) (Fig. 1e). We then compared the spontaneous firing rate between dSNc and vSNc DA neurons by plotting cumulative probability curves and performing a Kolmogorov–Smirnov (K–S) test. As illustrated in Fig. 1f, the curve for vSNc DA neurons was shifted to the right relative to that for dSNc DA neurons. This suggests that the overall spontaneous firing rate is higher in vSNc DA neurons than in dSNc DA neurons.

The magnitude of the increase in firing rate upon stimulation may represent the capacity of DA neurons to respond to input signals. To investigate whether dSNc and vSNc DA neurons differ in their response to stimuli, we performed whole-cell current-clamp recordings and injected neurons with steps of depolarizing current (2 s, 0–260 pA). Upon current injection, DA neurons exhibited elevated firing rates with or without adaptation (Fig. 1g). Similar proportions of dSNc DA neurons (83%, 19/23) and vSNc DA neurons (75%, 8/12) displayed adaptation in firing evoked by depolarizing stimuli ($x^2 = 0.41$, $P = 0.52$) (Fig. 1h). The adaptive DA neurons in the dSNc and vSNc displayed similar levels of spontaneous firing (Fig. 1i). Upon stimulation, the firing rates of dSNc and vSNc DA neurons increased with stimulation intensity, and the stimulus–response curves of the two groups of neurons largely overlapped (Fig. 1g, j). However, vSNc DA neurons reached a higher maximal firing rate than dSNc DA neurons (Mann–Whitney U Statistic = 24.500, $P = 0.006$) (Fig. 1j).

Aging nigrostriatal dopaminergic system and motor deficits
JP Fan et al.

865
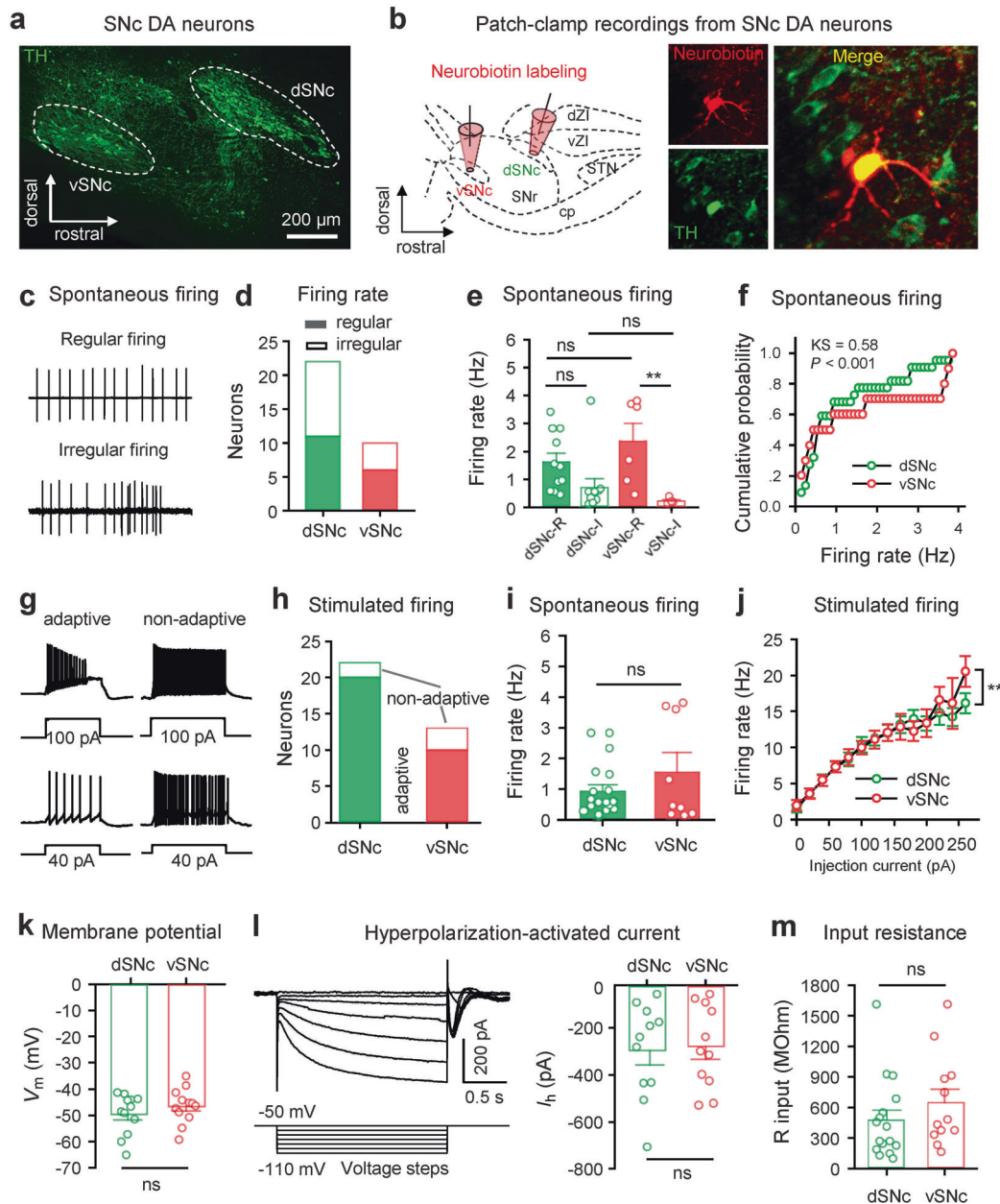
Fig. 1 Spontaneous and evoked firing in adult rat SNc DA neurons. Six-month-old Long-Evans rats were used for this set of experiments. **a** Visualization of dopaminergic (DA) neurons in a typical parasagittal midbrain section with immunostaining of tyrosine hydroxylase (TH) antibody (green). Clusters of DA neurons were located in the dorsal and ventral tiers of the substantia nigra pars compacta (dSNc, vSNc). **b** Patch-clamped neurons were filled with neurobiotin (red) and post hoc immunostaining with a TH-antibody was performed to identify DA neurons (green). **c** Spontaneous firing was recorded from SNc DA neurons with the patch-clamp technique in cell-attached mode. SNc DA neurons fired spontaneously in either a regular (upper panel) or irregular pattern (lower panel). **d** Stack plots show the number of neurons with a regular (solid box) or irregular (open box) firing pattern ($x^2 = 0.07$, $P = 0.80$). **e** Regular (solid bar) and irregular (open bar) firing rates in dSNc neurons (dSNc-R and dSNc-I) and vSNc DA neurons (vSNc-R and vSNc-I). $H = 15.59$, $P = 0.001$, Kruskal–Wallis one-way ANOVA. Pairwise multiple comparisons with the Holm–Sidak method: $q = 3.17$, $P = 0.009$, vSNc-R vs vSNc-I. **f** Cumulative probability curve of spontaneous firing rate in dSNc (green) and vSNc (red) neurons. Kolmogorov–Smirnov (K-S) test, KS = 0.58, $P < 0.001$. **g** Whole-cell current-clamp recordings from SNc DA neurons showed that depolarizing current injections elevated firing rates with (traces in the left panels) or without (traces in the right panels) adaptation in SNc DA neurons. **h** The number of adaptive (solid box) and nonadaptive (open box) DA neurons in the dSNc and vSNc ($P = 0.34$, Fisher Exact Test). **i** Spontaneous firing rate of adaptive dSNc and vSNc DA neurons ($T = 131.50$, $P = 0.98$, Mann–Whitney Rank Sum Test). **j** Upon depolarizing stimulation (0–260 pA), both dSNc DA neurons (green, $n = 17$) and vSNc DA neurons (red, $n = 9$) responded with increased firing rates. Maximal firing rate: $t = 2.81$, $P = 0.0097$, t-test. **k** Membrane potential of dSNc and vSNc DA neurons ($t = 1.01$, $P = 0.32$, two-tailed t-test). **l** Hyperpolarization-activated cation channel currents (I_h) in dSNc and vSNc DA neurons ($t = 0.20$, $P = 0.82$, two-tailed t-test). I_h was evoked by voltage steps from a holding potential of -50 mV to step potentials ranging from -50 to -110 mV with a 10 mV-decrement. The inward current following a voltage step was used to quantify I_h. **m** Input resistance of dSNc and vSNc DA neurons ($t = 1.10$, $P = 0.28$, two-tailed t-test). Input resistance was calculated from 5 mV hyperpolarizing step (500 ms)-induced baseline drift (pA) according to Ohm's law. In scatter plots, each circle represents a datum from one neuron. *$P < 0.05$; **$P < 0.01$; ns $P > 0.05$.

Aging nigrostriatal dopaminergic system and motor deficits
JP Fan et al.

866

As the membrane potential and hyperpolarization-activated cation channel current (Ih) critically affect spontaneous activity in midbrain DA neurons [40, 44], we compared these two parameters in dSNc and vSNc DA neurons. As illustrated in Fig. 1k, l, there was no significant difference in membrane potential or I_h between dSNc and vSNc DA neurons. Although according to Ohm's law, the current-injection-induced membrane response likely depends on the input resistance of the membrane, we observed no difference in input resistance between dSNc and vSNc DA neurons (Fig. 1m).

Therefore, in young adult rats, vSNc DA neurons displayed higher spontaneous firing rates and were more responsive to strong stimulation than dSNc DA neurons, but the underlying biophysical bases for these features warrant further investigation.

Age-dependent changes in dSNc and vSNc DA neurons

We next examined whether the activity of SNc DA neurons changes with age. We performed patch-clamp recordings on both dSNc and vSNc neurons in brain slices from 6-, 12-, and 24-month-old rats. As firing pattern is an important parameter associated with neuronal function, we compared the proportion of dSNc DA neurons displaying an irregular firing pattern, and found no significant differences among 6-, 12-, and 24-month-old rats (Fig. 2a). We then pooled dSNc DA neurons with either regular or irregular firing patterns together. We observed that the spontaneous firing rate in dSNc DA neurons from 12-month-old rats was significantly higher than that from 6- and 24-month-old rats (Fig. 2b). Similarly, the proportion of vSNc DA neurons exhibiting an irregular firing pattern did not differ among 6-month-old (40%, 4/10), 12-month-old (12.5%, 2/16), and 24-month-old (22.2%, 2/9) rats (Fig. 2c), and the spontaneous firing rate in vSNc DA neurons from 12-month-old rats was higher than that from 6- and 24-month-old rats (Fig. 2d). In contrast to the results from dSNc DA neurons, vSNc DA neurons from 24-month-old rats fired faster than those from their 6-month-old counterparts (Fig. 2b, d).

As illustrated in Fig. 1h, upon depolarizing stimuli, most dSNc DA neurons from 6-month-old rats showed accelerated firing with adaptation. A similar phenomenon was observed in dSNc DA neurons from 12- and 24-month-old rats (Fig. 2e). As only a limited number of dSNc DA neurons showed nonadaptive firing, we further analyzed the relationship between firing rate and stimulation intensity in adaptive dSNc DA neurons only. We found that dSNc DA neurons from 12- and 24-month-old rats responded more strongly to stimuli than those from 6-month-old rats (Fig. 2f). Consistent with this, the maximal firing rate of dSNc DA neurons increased significantly with age, from 6-, to 24-, to 12-months old (Fig. 2g).

Similar to dSNc DA neurons, the proportion of vSNc DA neurons showing adaptive firing remained the same across ages (Fig. 2h). The maximal response of vSNc DA neurons to depolarizing stimulation (maximal firing rate) was enhanced with age (Fig. 2i, j), with a somewhat different trend from that observed in dSNc DA neurons.

In summary, dSNc and vSNc DA neurons exhibit different age-dependent variations in spontaneous firing rate and stimulation-evoked firing rate.

Age-dependent changes in biophysical properties in SNc DA neurons

We next tested whether aging differentially affects the membrane properties of dSNc and vSNc DA neurons, including membrane potentials, Ih, and input resistance. In dSNc DA neurons, neither membrane potential nor input resistance showed statistically significant age-dependent changes (Fig. 3a, b); however, I_h was significantly reduced in the 12-month-old group (Fig. 3c). In vSNc DA neurons, age did not affect membrane potential (Fig. 3d), input resistance (Fig. 3e), or I_h (Fig. 3f). Therefore, the age-dependent changes in spontaneous and stimulated firing in dSNc and vSNc DA neurons may be associated with age-related modifications of

ion channels that do not affect membrane potential or input resistance but that modulate firing in DA neurons. Large-scale screening investigations are warranted to test this possibility.

Age-dependent changes in locomotion and coordination

Since DA neurons regulate various aspects of motor behavior [20, 40, 41, 45–47], we hypothesized that the age-dependent alterations in SNc DA neurons may parallel changes in motor functions.

To examine locomotor behaviors in rats at different ages, we allowed rats to freely explore in an open field arena (Fig. 4a) for 30 min and analyzed their locomotion in both exploratory (first 5 min) and habituated (last 5 min) stages. In the exploratory stage, the distance the rats traveled increased significantly in 12- and 18-month-old rats, relative to 6-month rats (Fig. 4b), but declined in 24-month-old rats (Fig. 4b). In the habituated stage, the distances traveled were reduced to the same level in all age groups (Fig. 4c). As 18-month-old rats were the most active in the exploratory stage, they showed a more prominent reduction in their vigor of movement in the habituated stage than 6-month-old rats (Fig. 4d). Our results suggest that 12- and 18-month-old rats exhibit higher levels of exploratory locomotion.

To examine age-related changes in subjects' limb coordination, rats were tested on a narrow balance beam of restricted length, such that they were able to move back and forth in a few steps (Fig. 4e). Thus, this apparatus minimizes the confounding effects of locomotor and exploratory drive on coordination. We observed that 18- and 24-month-old rats stayed on the beam for significantly shorter durations than 6-month-old rats (Fig. 4e). We also used a cylinder test to examine limb coordination. Compared with 6-month-old rats, the older rats spent less time rearing, a behavior representing the ability of rats to coordinate limbs for postural balance (Fig. 4f). These data suggest that limb coordination declines in rats older than 12 months.

Fig. 4 shows that aging affects both locomotion and coordination in rats. We wondered whether aging has similar effects in mice. We thus tested mice aged 6 months, 12 months, 18 months, and 24 months in the open field test, beam walking test, and rotarod test.

In the exploratory stage, 12-month-old mice showed hyperactivity in an open field arena, relative to other ages (Fig. 5a). The hyperactive 12-month-old mice showed higher mobility (Fig. 5b) and moving velocity (Fig. 5c) than 6- and 24-month-old mice. In the habituated stage, 6- and 12-month-old mice were more active than 18- and 24-month-old mice (Fig. 5d). Compared with the 6-month-old mice, 12-, 18-, and 24-month-old mice had a significantly greater reduction in activity after habituation (Fig. 5e). The data indicate that mice have enhanced exploratory behavior (increased mobility and moving velocity) at 12 months, and are less active after habituation at 18 and 24 months.

The performance of 24-month-old mice in the beam walking test was worse than the performance of younger mice. Specifically, the older mice spent significantly longer latency traversing the beam (Fig. 5f) and experienced more slips as they walked across the beam (Fig. 5g). In the rotarod test, 18- and 24-month-old mice stayed on the rotarod for a shorter duration than the younger mice when it was rotating at gradually accelerating speeds (Fig. 5h). The maximal rotation speed at which 18- and 24-month-old mice could balance was lower than that for 6- and 12-month-old mice (Fig. 5i). These data show that mice exhibit an age-dependent decline in coordination.

Our behavioral data show that 12- and 18-month-old rats and 12-month-old mice exhibit locomotor hyperactivity relative to 6-month-old and 24-month-old rats and mice, and that 18- and 24-month-old rats and mice have deficits in balance and coordination.

Age-dependent changes in the survival of SNc DA neurons and striatal DA terminals

We next tested whether aging differentially affects dSNc and vSNc DA neurons in mice. Consistent with previous studies [4, 22], we

Aging nigrostriatal dopaminergic system and motor deficits
JP Fan et al.

867
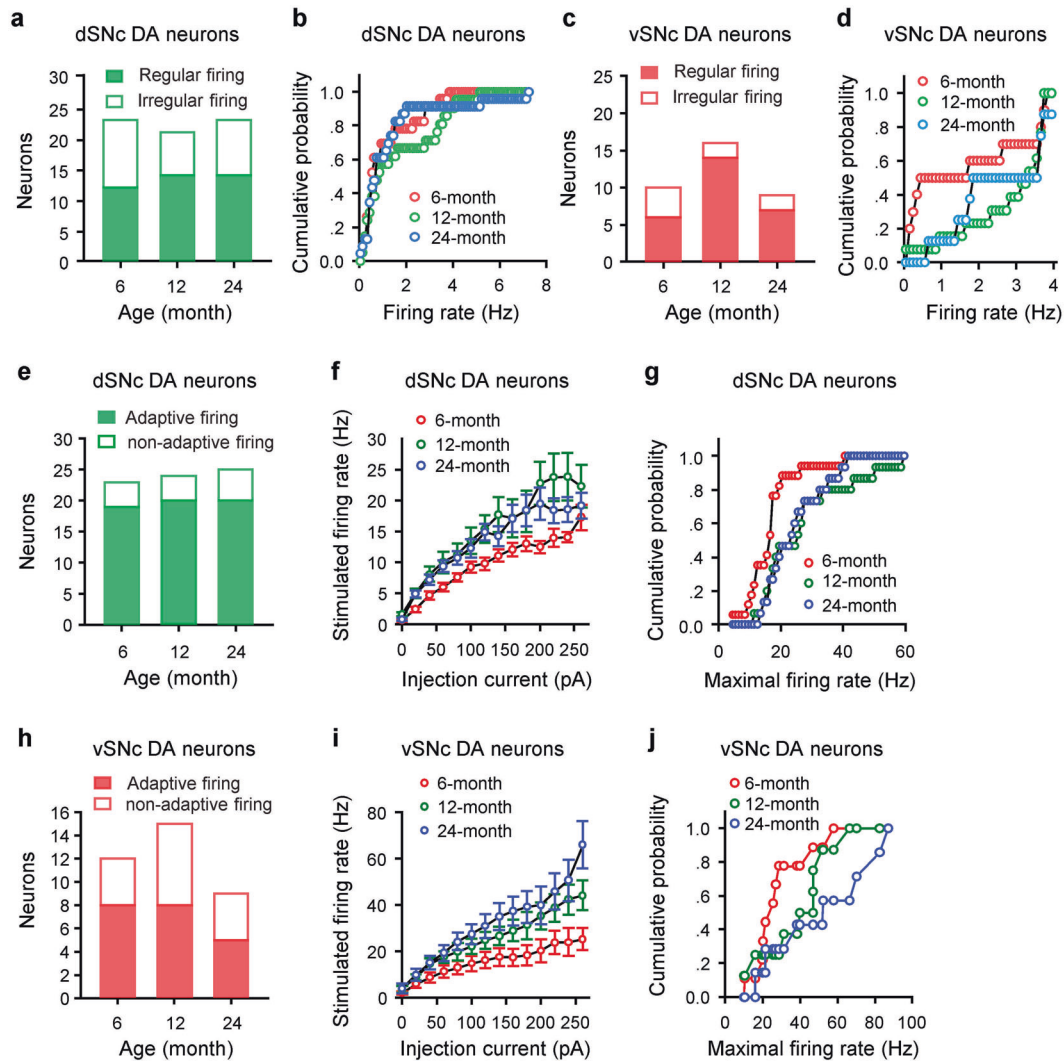
Fig. 2 Age-dependent changes in spontaneous and evoked firing of rat SNc DA neurons. a Number of dSNc DA neurons showing regular and irregular firing patterns in 6-, 12-, and 24-month-old rats ($x^2 = 0.98$, $P = 0.61$, chi-square test). **b** Cumulative probability curve of spontaneous firing of dSNc DA neurons in 6-, 12-, and 24-month-old rats (KS = 0.49, $P = 0.0002$, 6-month vs 12-month; KS = 0.26, $P = 0.15$, 6-month vs 24-month; KS = 0.54, $P < 0.0001$, 12-month vs 24-month). **c** Number of vSNc DA neurons showing regular and irregular firing patterns in 6-, 12-, and 24-month-old rats ($x^2 = 2.64$, $P = 0.27$). **d** Cumulative probability curves of spontaneous firing rate of vSNc DA neurons in 6-, 12-, and 24-month-old rats (KS = 0.76, $P < 0.0001$, 6-month vs 12-month; KS = 0.5, $P = 0.0002$, 6-month vs 24-month; KS = 0.39, $P = 0.005$, 12-month vs 24-month). **e** Upon current injection, whole-cell current-clamped dSNc DA neurons showed either an adaptive (solid box) or nonadaptive (open box) firing pattern ($x^2 = 0.102$, $P = 0.95$). **f** Depolarizing current injection-evoked firing in dSNc DA neurons from 6-, 12-, and 24-month-old rats. **g** Cumulative probability curves of maximal evoked firing rates in dSNc DA neurons from 6-, 12-, and 24-month-old rats (KS = 0.59, $P < 0.001$, 6-month vs 12-month; KS = 0.34, $P = 0.003$, 6-month vs 24-month; KS = 0.32, $P = 0.006$, 12-month vs 24-month). **h** Upon current stimuli, current-clamped vSNc DA neurons showed either an adaptive (solid box) or nonadaptive (open box) firing pattern ($x^2 = 0.53$, $P = 0.77$). **i** Depolarizing current injection-evoked firing in vSNc DA neurons from 6-, 12-, and 24-month-old rats. **j** Cumulative probability curves of maximal stimulated firing rates in vSNc DA neurons from 6-, 12-, and 24-month-old rats (KS = 0.29, $P = 0.26$, 6-month vs 12-month; KS = 0.50, $P = 0.005$, 6-month vs 24-month; KS = 0.25, $P = 0.44$, 12-month vs 24-month).

confirmed the loss of dSNc DA neurons in 18- and 24-month-old mice, but not in 12-month-old mice (Fig. 6a, b). Similar to dSNc DA neurons, vSNc DA neurons decreased in number in 18- and 24-month-old mice (Fig. 6c, d). We also performed TH-staining in the dorsal striatum to image DA axonal fibers and terminals (Fig. 6e). The intensity of TH-positive structures in the dorsal striatum was significantly lower in 12-, 18-, and 24-month-old mice than in 6-month-old mice (Fig. 6e, f).

The nigrostriatal DA system originates from SNc DA neurons and innervates the dorsal striatum. Given that the survival and activity of dSNc and vSNc DA neurons and DA fibers in the dorsal striatum are altered in an age-dependent manner (Figs. 2 and 6a–f), we wondered whether dopamine release in the dorsal striatum also
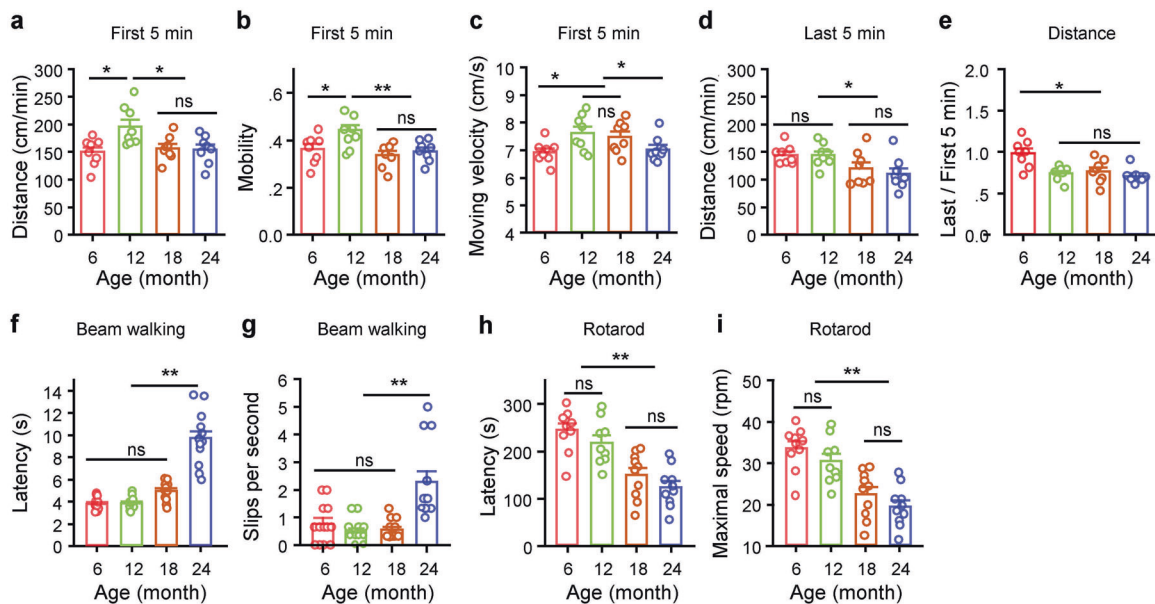
varies with age. To measure dopamine release, we used a viral vector to transfect a dopamine sensor (AAV-hSyn-GRAB-DA3.3) [30] into the dorsal striatum (Fig. 7a). Under an epi-fluorescence microscope, we observed that an electrical stimulation pulse evoked a robust increase in fluorescence intensity in striatal slices expressing GRAB-DA3.3 (Fig. 7b). We quantified dopamine release as the fold increase in fluorescence intensity following electrical stimulation (Fig. 7c). We stimulated striatal slices with one electrical pulse (1 P) and five electrical pulses (5 P) at 1, 5, 25, and 50 Hz [48], and observed that electrical-stimulation-evoked dopamine release in striatal slices differed in amplitude between 6- and 22-month-old mice (Fig. 7c). We next compared the peak amplitude of dopamine release upon various stimulation paradigms among 6-, 12-, and

Aging nigrostriatal dopaminergic system and motor deficits
JP Fan et al.

868
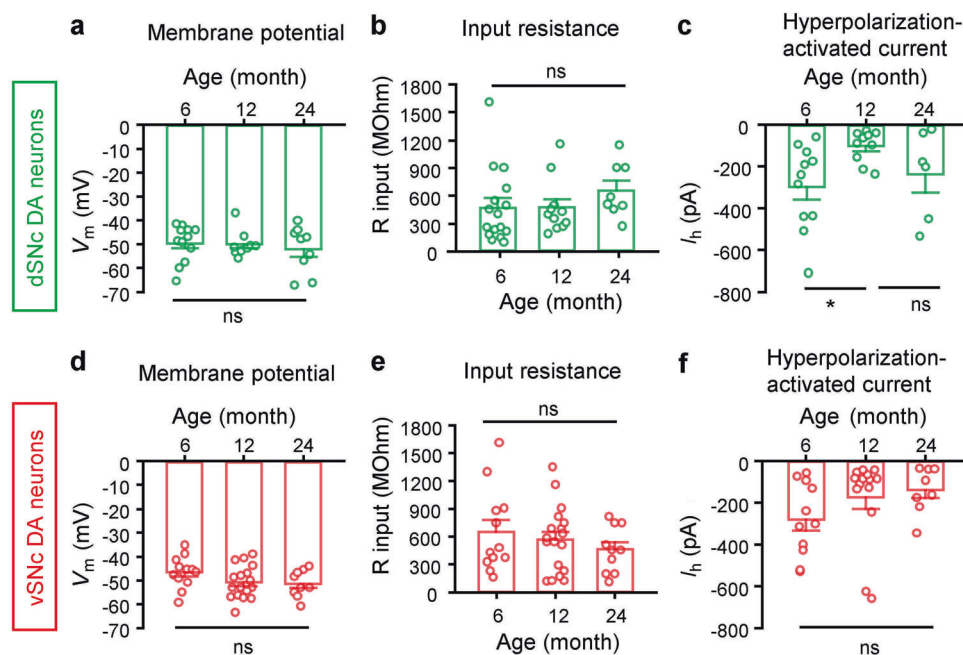
Fig. 3 Age-dependent changes in membrane properties of dSNc and vSNc DA neurons. Whole-cell current-clamp recordings were performed to record membrane potential, input resistance, and the hyperpolarization-activated cation channel current (Ih) from dSNc and vSNc DA neurons in parasagittal midbrain slices from 6-, 12- and 24-month-old rats. Neither membrane potential (**a**) nor input resistance (**b**) were altered in dSNc DA neurons during aging (V_m: $F_{(2, 34)} = 0.29$, $P = 0.75$, one-way ANOVA; R input: $H = 4.01$, $P = 0.14$, Kruskal–Wallis one-way ANOVA on Ranks). **c** I_h was reduced at 12 months of age in dSNc DA neurons ($F_{(2, 34)} = 3.62$, $P = 0.04$, one-way ANOVA; $t = 2.66$, $P = 0.04$, 6 vs 12 months). The membrane potential (**d**), input resistance (**e**), and I_h (**f**) in vSNc DA neurons did not change with age. **d** $F_{(2, 35)} = 1.9$, $P = 0.16$, one-way ANOVA. **e** $F_{(2, 35)} = 0.92$, $P = 0.63$, one-way ANOVA. **f** $H = 4.17$, $P = 0.13$, Krukal–Wallis one-way ANOVA on ranks. Each circle represents a datum from one neuron. dSNc: 6-month, $n = 16$; 12-month, $n = 12$; 24-month, $n = 9$. vSNc: 6-month, $n = 12$; 12-month, $n = 17$; 24-month, $n = 9$. *$P < 0.05$.
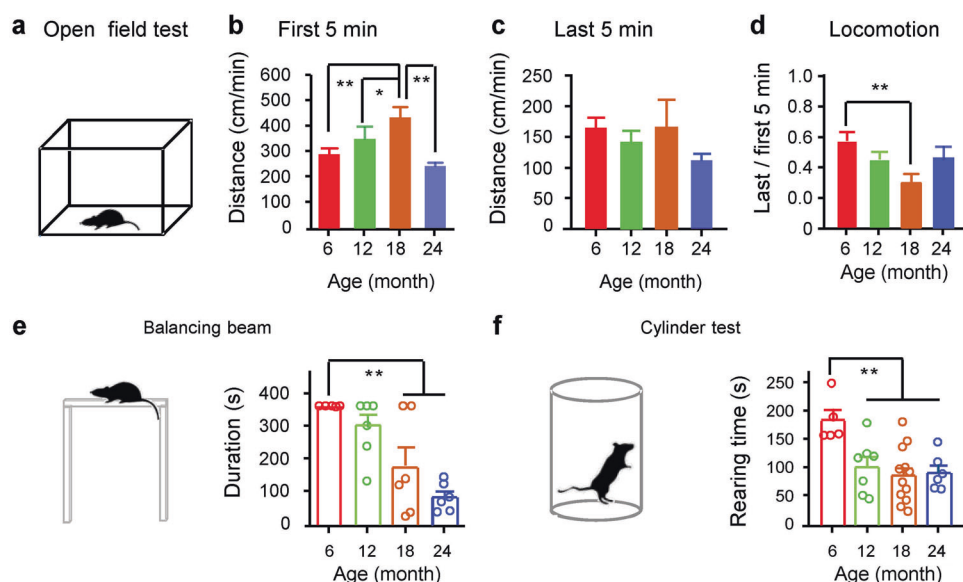
Fig. 4 Age-dependent changes in locomotion and coordination in rats. a Rats were placed in an open field arena and their locomotor behavior was examined for 30 min. **b** Summary of distance (cm/min) traveled by the rats in the first 5 min ($F_{(3, 29)} = 8.2$, $P < 0.001$, one-way ANOVA; pairwise comparison with Student–Newman–Kerl (SNK) method; 6-month: $n = 10$, 12-month: $n = 9$, 18-month: $n = 8$, 24-month: $n = 6$). **c** Summary of distance (cm/min) traveled in the last 5 min ($F_{(3, 29)} = 0.61$, $P = 0.61$, one-way ANOVA; 6-month: $n = 10$, 12-month: $n = 9$, 18-month: $n = 8$, 24-month: $n = 6$). **d** The distance traveled during the last 5 min was quantified as a percentage of the distance traveled during the first 5 min ($F_{(3, 29)} = 4.65$, $P = 0.009$, one-way ANOVA; $q = 5.28$, $P = 0.005$, 6-month vs. 18-month, pairwise comparison with Dunn's method). **e** Time on a short balancing beam ($F_{(3, 29)} = 11.71$, $P < 0.001$, one-way ANOVA). **f** Time spent rearing in a cylinder ($F_{(3, 29)} = 5.60$, $P = 0.004$, one-way ANOVA). In (**e**, **f**), pairwise comparisons were conducted with SNK methods. *$P < 0.05$; **$P < 0.01$; ns $P > 0.05$.

Aging nigrostriatal dopaminergic system and motor deficits
JP Fan et al.

869

Fig. 5 **Age-dependent changes in locomotion and coordination in mice. a** Twelve-month-old mice showed enhanced locomotion during the first 5 min in an open field arena, compared with other age groups ($F_{(3, 28)} = 4.82$, $P = 0.008$, one-way ANOVA) (pairwise comparison with SNK method: $t = 3.35$, $P = 0.01$, 6- vs 12- month; $t = 2.85$, $P = 0.03$, 12- vs 18-month; $t = 3.03$, $P = 0.03$, 12- vs 24-month). **b** Mobility of mice during the first 5 min in the open field arena ($F_{(3, 28)} = 5.30$, $P = 0.006$, one-way ANOVA) (pairwise comparison with SNK method: $t = 2.86$, $P = 0.03$, 6- vs 12-month; $t = 3.71$, $P = 0.006$, 12- vs 18-month; $t = 3.05$, $P = 0.026$, 12- vs 24-month). **c** Moving velocity of mice during the first 5 min in the open field arena ($F_{(3, 28)} = 4.95$, $P = 0.014$, one-way ANOVA) (pairwise comparison with SNK method: $t = 2.78$, $P = 0.05$, 6- vs 12- and 18-month; $t = 2.4$, $P = 0.05$, 12- and 18-month vs 24-month). **d** Distance traveled in the last 5 min in an open field arena was recorded from 6-, 12-, 18-, and 24-month-old mice ($F_{(3, 28)} = 3.69$, $P = 0.02$) (pairwise comparison with SNK method: $t = 3.32$, $P = 0.003$, 6- and 12-month vs 18- and 24-month). **e** Ratio of distance traveled in the last 5 min relative to distance traveled in the first 5 min in the open field arena ($F_{(3, 28)} = 8$, $P < 0.001$, one-way ANOVA) (pairwise comparison with SNK method: $t = 3.88$, $P = 0.003$, 6- vs 12-month; $t = 3.54$, $P = 0.006$, 6- vs 18-month; $t = 4.40$, $P < 0.001$, 6- vs 24-month). **f** Time latency for mice to walk across the beam ($F_{(3, 34)} = 7.24$, $P = 0.0004$) (Tukey's multiple comparisons test: $q = 16.3$, $P < 0.0001$, 6- vs 24-month; $q = 16.05$, $P < 0.0001$, 12- vs 24-month; $q = 13.12$, $P < 0.0001$, 18- vs 24-month). **g** Slips made by mice as they traversed the beam ($F_{(3, 34)} = 13.93$, $P < 0.0001$, one-way ANOVA) (Tukey's multiple comparisons test: $q = 6.67$, $P = 0.0001$, 6- vs 24-month; $q = 7.92$, $P < 0.0001$, 12- vs 24-month; $q = 7.59$, $P < 0.0001$, 18- vs 24-month). **h** Latency for mice to fall from a rotarod with accelerating rotation ($F_{(3, 34)} = 15.19$, $P < 0.0001$, one-way ANOVA) (Tukey's multiple comparisons test: $q = 6.59$, $P = 0.0002$, 6- vs 18-month; $q = 8.35$, $P < 0.0001$, 6- vs 24-month; $q = 4.62$, $P = 0.012$, 12- vs 18-month; $q = 6.33$, $P = 0.0004$, 12- vs 24-month). **i** Maximal rotation speed of the rotarod when mice fell off. As maximal speed is a function of latency, the statistical results among age groups are the same as those in (**h**). **a**–**e** 6-month, $n = 8$; 12-month, $n = 8$; 18-month, $n = 8$; 24-month, $n = 8$. **f**–**i** 6-month, $n = 9$; 12-month, $n = 9$; 18-month, $n = 10$; 24-month, $n = 10$. *$P < 0.05$; **$P < 0.01$; ns $P > 0.05$.

22-month-old mice. As illustrated in Fig. 7d, the dopamine release evoked by 1 P was significantly reduced in 12- and 22-month-old mice relative to 6-month-old mice; with 5 P at frequencies ≥5 Hz, dopamine release in 12-month-old mice reached the level released in 6-month-old mice, and was significantly greater than the level in 22-month-old mice; dopamine release upon 1 P and 5 P was significantly lower in 22-month-old mice than in 6- and 12-month-old mice. These results suggest that dopamine release is impaired in 12- and 22-month-old mice and that increasing stimulation frequency can restore dopamine release in 12-month-old mice, but not in 22-month-old mice.

To test whether repetitive-stimulation-induced accumulation of dopamine varies with age, we divided the amplitudes of responses evoked by 5 P with those evoked by 1 P and compared the ratios in 6-, 12-, and 22-month-old mice. Fig. 7e shows that, in 12- and 22-month-old mice, 5 P at 25 and 50 Hz caused significant accumulation of dopamine release. In studies measuring dopamine levels with voltammetry, the difference between multiple-stimuli-induced peak responses and single-stimulus-induced responses is used to evaluate release probability:[49] a larger difference corresponds to lower release probability, and vice versa. Our data suggest that dopamine release probability is reduced in 12- and 22-month-old mice. As shown in Fig. 7f, the kinetics of 1 Hz 5 P-induced dopamine release differed markedly among 6-, 12-, and 22-month-old mice: in 12- and 22-month-old mice, the responses to each electrical stimulus were discernable, but were

relatively obscured in 6-month-old mice. When we normalized the peak responses induced by 5 P to the 1 P response, we observed that peak responses decayed faster in 6- and 12-month-old mice than in 22-month-old mice (Fig. 7g). This result suggests that a more severe impairment in dopamine release may occur in aged mice. We postulate that in 22-month-old mice, dopamine release may be severely inhibited: an electrical stimulus evokes less dopamine release, leaving more active vesicles to be recruited by the next stimulus; however, in 6- and 12-month-old mice, the initial electrical stimulus evokes greater dopamine release, resulting in fewer active vesicles remaining to be recruited by the next stimulus.

These results demonstrate that dopamine release is impaired in 12- and 22-month-old mice; in 12-month-old mice, dopamine release can be restored by higher frequency stimulation but increasing stimulation frequency cannot compensate for the deficit in 22-month-old mice.

Elevating dopamine levels rescues the age-dependent deterioration in locomotion and coordination
As our data reveal age-dependent alterations in both the nigrostriatal DA system and motor function in rodents, to understand whether the deficits in the former are associated with alterations in the latter, we systemically administered a dopamine transporter inhibitor, GBR12935 (GBR), in mice. We observed that, in all age groups, GBR significantly enhanced locomotion in the

Aging nigrostriatal dopaminergic system and motor deficits
JP Fan et al.

870
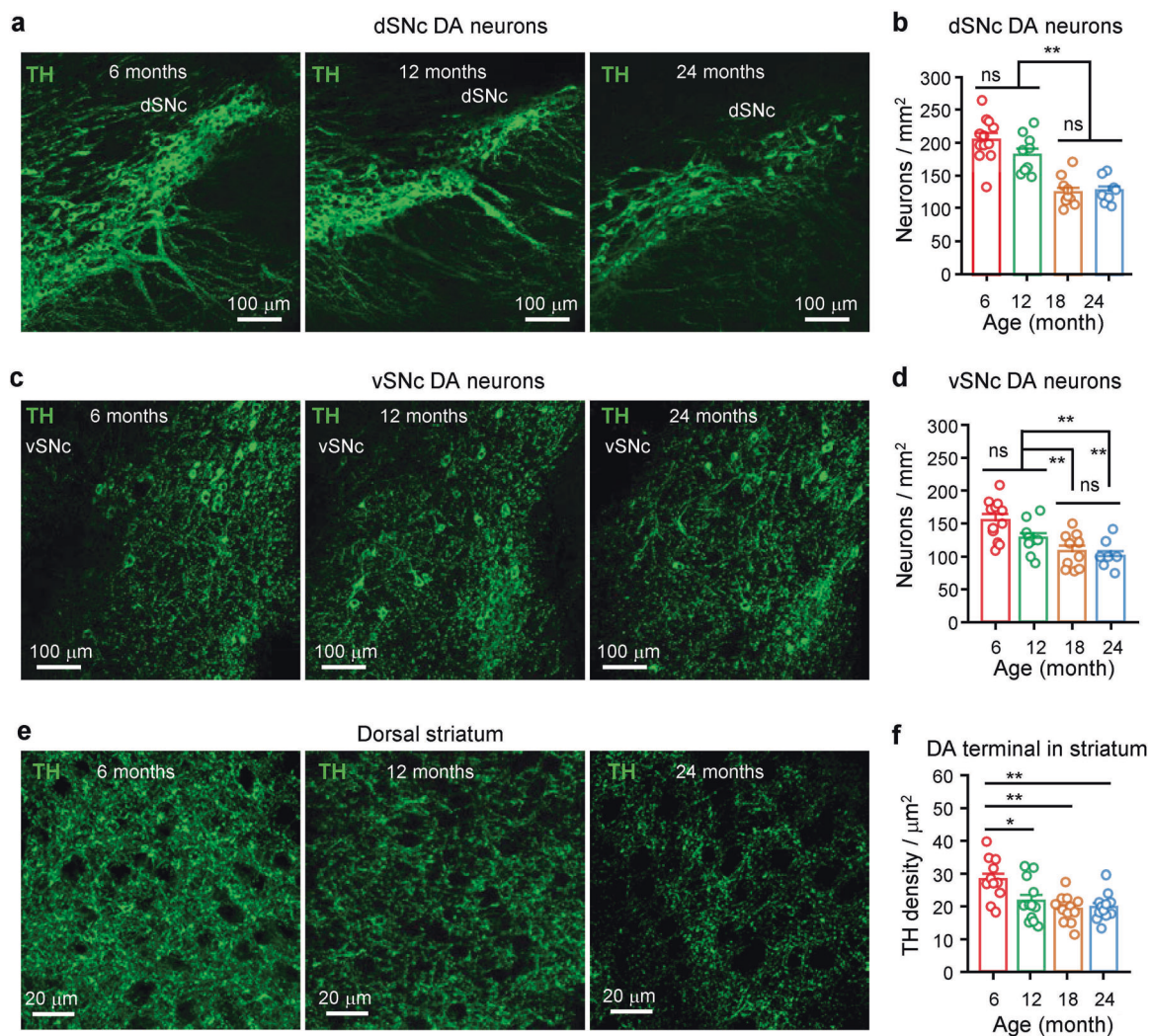
Fig. 6 Age-dependent alterations in SNc DA neurons and striatal DA terminals in mice. 6-, 12-, 18-, and 24-month-old mice were sacrificed. Immunohistochemistry with a TH antibody was performed to label DA neurons in the dSNc and vSNc and DA terminals in the dorsal striatum. **a** Typical images showing TH-positive neurons (green) in the dSNc of 6-, 12-, and 24-month-old mice. **b** 18- ($n = 8$) and 24-month-old ($n = 8$) mice exhibited fewer dSNc DA neurons than 6- ($n = 12$) and 12-month-old ($n = 9$) mice. $F_{(3, 33)} = 21.72$, $P < 0.001$, one-way ANOVA. $t = 2.04$, $P = 0.10$, 6-month vs 12-month; $t = 6.82$, $P < 0.001$, 6-month vs 18-month; $t = 6.19$, $P < 0.001$, 6-month vs 24-month; $t = 4.58$, $P < 0.001$, 12-month vs 18-month; $t = 4.11$, $P < 0.001$, 12-month vs 24-month; $t = 0.2$, $P = 0.84$, 18-month vs 24-month, pairwise multiple comparisons with the Holm–Sidak method. **c** Typical images showing TH-positive neurons (green) in the vSNc of 6-, 12-, and 24-month-old mice. **d** 18- ($n = 10$) and 24-month-old ($n = 7$) mice exhibited fewer vSNc DA neurons than 6-month-old mice. $F_{(3, 33)} = 8.85$, $P < 0.001$, one-way ANOVA. $t = 2.47$, $P = 0.07$, 6-month vs 12-month; $t = 4.52$, $P < 0.001$, 6-month vs 18-month; $t = 4.19$, $P < 0.001$, 6-month vs 24-month; $t = 1.65$, $P = 0.21$, 12-month vs 18-month; $t = 2.12$, $P = 0.12$, 12-month vs 24-month; $t = 0.57$, $P = 0.57$, 18-month vs 24-month, pairwise multiple comparisons with the Holm–Sidak method. **e** Typical images showing TH-positive structures (green) in the dorsal striatum of 6-, 12-, and 24-month-old mice. **f** Fluorescence intensity of TH-staining declined in 12- ($n = 12$), 18- ($n = 12$), and 24-month-old ($n = 12$) mice, relative to that in 6-month-old ($n = 11$) mice. $F_{(3, 43)} = 7.21$, $P < 0.001$, one-way ANOVA. $t = 3.06$, $P = 0.015$, 6-month vs 12-month; $t = 4.13$, $P < 0.001$, 6-month vs 18-month; $t = 3.86$, $P = 0.002$, 6-month vs 24-month; $t = 1.08$, $P = 0.64$, 12-month vs 18-month; $t = 0.81$, $P = 0.67$, 12-month vs 24-month, pairwise multiple comparisons with the Holm–Sidak method. Images in **a** and **c** were taken through a 20× objective (NA: 0.80), and those in **e** were taken through a 63× oil lens (NA: 1.40).

exploratory stage (Fig. 8a) and increased mobility (Fig. 8b), but did not affect moving velocity (Fig. 8c). In the habituated stage, GBR also significantly enhanced locomotion (Fig. 8d). It did not affect the ratio of locomotion in the habituated and exploratory stages (Fig. 8e). In the beam walking test, GBR significantly accelerated the crossing time (Fig. 8f), but did not improve slipping (Fig. 8g) in 18- and 24-month-old mice. In the rotarod test, GBR increased the duration that 18- and 24-month-old mice stayed on the rotarod (Fig. 8h) and the maximal rotation speed at which they could balance (Fig. 8i). Overall, GBR enhanced locomotion in all age groups but improved coordination more prominently in 18- and 24-month-old mice.

These data hint that the age-related alterations in the nigrostriatal DA system may be associated with age-dependent changes in locomotion and coordination.

Relationship between age-dependent alterations in the nigrostriatal DA system and motor functions

We summarized age-dependent alterations in spontaneous and evoked firing in SNc DA neurons (Fig. 9a, b), survival of SNc DA neurons (Fig. 9c), dopamine release in the striatum (Fig. 9d), locomotion (Fig. 9e) and coordination (Fig. 9f) in rats, and locomotion (Fig. 9g) and coordination (Fig. 9h) in mice. To facilitate comparison of parameters among groups and visualize

Aging nigrostriatal dopaminergic system and motor deficits
JP Fan et al.

871
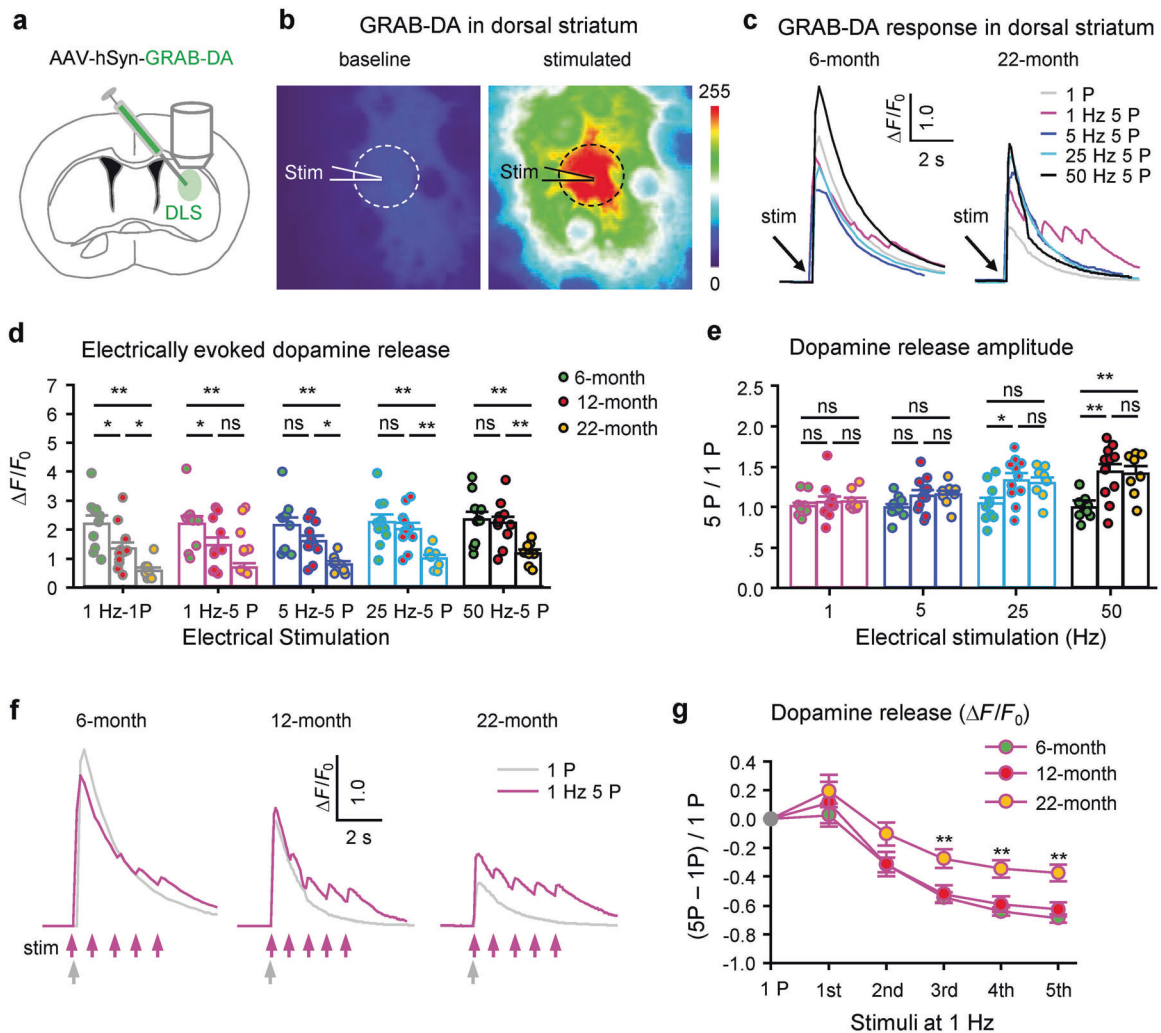
Fig. 7 Age-dependent alterations in striatal dopamine release in mice. a AAV-hSyn-GRAB-DA3.3 was microinjected in the dorsal striatum of 6-, 12-, and 22-month-old mice. **b** Striatal slices were prepared 3 weeks after viral injection. Heatmaps showing fluorescence intensity of GRAB-DA before (baseline) and after electrical stimulation (stimulated); an area around the tip of the stimulating electrode was marked to quantify dopamine release. **c** Typical traces showing dopamine release evoked by 1 pulse (1 P) and 5 pulses (5 P) (at 1, 5, 25, and 50 Hz) of electrical stimuli in striatal slices from a 6-month-old mouse (left) and a 22-month-old mouse (right). **d** Electrically evoked dopamine release in striatal slices from 6-, 12-, and 22-month-old mice. 1 P: $F_{(2, 27)} = 11.12$, $P < 0.001$; 1 Hz 5 P: $F_{(2, 27)} = 8.86$, $P = 0.001$; 5 Hz 5 P: $F_{(2, 27)} = 9.58$, $P < 0.001$; 25 Hz 5 P: $F_{(2, 27)} = 8.23$, $P = 0.002$; 50 Hz 5 P: $F_{(2, 27)} = 6.99$, $P = 0.004$. **e** The ratios of dopamine release evoked by 5 P (at 1, 5, 25, and 50 Hz) to that evoked by 1 P were calculated and compared across 6-, 12-, and 22-month-old mice. 1 Hz: $F_{(2, 27)} = 0.37$, $P = 0.69$; 5 Hz: $F_{(2, 27)} = 2.46$, $P = 0.11$; 25 Hz: $F_{(2, 27)} = 4.37$, $P = 0.02$; 50 Hz: $F_{(2, 27)} = 7.96$, $P = 0.002$. **f** Typical traces showing dopamine release evoked by 1 P (gray) and 5 P (purple) at 1 Hz. **g** The peak dopamine release evoked by each of the five individual pulses was gradually reduced in 6-, 12-, and 22-month-old mice. First pulse: $F_{(2, 27)} = 0.57$, $P = 0.57$; second pulse: $F_{(2, 27)} = 2.62$, $P = 0.09$; third pulse: $F_{(2, 27)} = 7.38$, $P = 0.003$; fourth pulse: $F_{(2, 27)} = 10.19$, $P = 0.0005$; fifth pulse: $F_{(2, 27)} = 12.34$, $P = 0.0002$. Circles in (**d**, **e**, **g**): 6-month, solid green, $n = 10$; 12-month, solid red, $n = 11$; 22-month, solid orange, $n = 9$. *$P < 0.05$; **$P < 0.01$; ns $P > 0.05$.

the relationship of age-dependent alterations across parameters, we normalized all data to the averages in 6-month-old animals. Spontaneous and evoked firing in SNc DA neurons and locomotion in rats and mice showed reverse V-shaped changes with age, while survival of SNc DA neurons, peak dopamine release, and coordination in both rats and mice declined with age. Our correlation analysis in the mouse aging cohort shows that the number of dSNc and vSNc DA neurons was significantly correlated with locomotion and coordination, while the density of TH-positive fibers and terminals in the striatum was correlated with beam-walking performance, but not locomotion (Table 1). These results support the hypothesis that the activity of SNc DA neurons and striatal dopamine release differentially regulate locomotion and coordination.

DISCUSSION
Although accumulating evidence implicates age-related alterations in the nigrostriatal DA system in motor dysfunctions in aged subjects, there is a lack of sophisticated functional studies designed to investigate the associations between age-related changes in individual anatomical components of the nigrostriatal DA system and particular motor phenotypes. Here, we employed multidisciplinary techniques to record the activity of dSNc and vSNc DA neurons, to measure the release of dopamine from striatal DA terminals, and to analyze locomotion and coordination in rodents. In this study, we established aging cohorts comprising 6−24-month-old rodents, covering young adult (~6 months), early middle age (~12 months), late middle age (~18 months), and old age (~24 months). These aging cohorts allowed us to reveal

Aging nigrostriatal dopaminergic system and motor deficits
JP Fan et al.

872
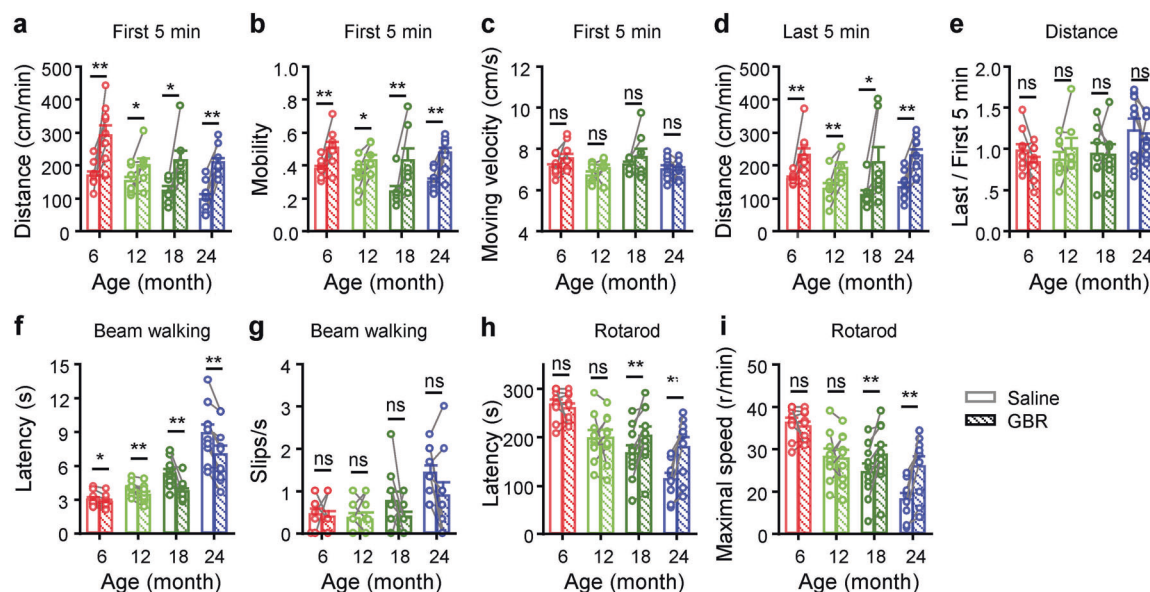
Fig. 8 Dopamine transporter inhibitor improves movement in mice. Open field, balancing beam, and rotarod tests were used to examine motor function in 6- ($n = 9$), 12- ($n = 7$), 18- ($n = 7$), and 24-month-old ($n = 9$) mice. The mice were subjected to intraperitoneal injection of saline and GBR 12935 (a dopamine transporter inhibitor, GBR, 10 mg/kg). **a** Distance during the first 5 min in the open field arena. $F_{(1, 30)} = 48.99$, $P < 0.0001$, Saline vs GBR; $F_{(3, 28)} = 2.95$, $P = 0.06$, among ages, two-way repeated-measures ANOVA. **b** Mobility in the first 5 min in the open field arena. $F_{(1, 30)} = 35.632$, $P < 0.001$, Saline vs GBR; $F_{(3, 28)} = 1.76$, $P = 0.19$, among ages, two-way repeated-measures ANOVA. **c** Moving velocity in the first 5 min in the open field arena. $F_{(1, 30)} = 1.30$, $P = 0.30$, Saline vs GBR; $F_{(3, 28)} = 1.31$, $P = 0.30$, among ages, two-way repeated-measures ANOVA. **d** Distance during the last 5 min in the open field arena. $F_{(1, 30)} = 17.34$, $P = 0.006$, Saline vs GBR; $F_{(3, 28)} = 0.78$, $P = 0.52$, among ages, two-way repeated-measures ANOVA. **e** Ratio of distance during the last 5 min to the first 5 min in the open field arena. $F_{(1, 30)} = 0.02$, $P = 0.89$, Saline vs GBR; $F_{(3, 28)} = 1.40$, $P = 0.28$, among ages, two-way repeated-measures ANOVA. **f** Latency to walk across the beam. $F_{(1, 30)} = 41.60$, $P < 0.0001$, Saline vs GBR; $F_{(3, 28)} = 30.83$, $P < 0.0001$, among ages, two-way repeated-measures ANOVA. **g** Slips from the beam. $F_{(1, 30)} = 4.55$, $P = 0.07$, Saline vs GBR; $F_{(3, 28)} = 4.38$, $P = 0.01$, among ages, two-way repeated-measures ANOVA. **h** Latency to fall from rotarod. $F_{(1, 30)} = 13.82$, $P = 0.006$, Saline vs GBR; $F_{(3, 28)} = 10.24$, $P < 0.001$, among ages, two-way repeated-measures ANOVA. **i** Maximal rotation speed of the rotarod when mice fell off. $F_{(1, 30)} = 12.52$, $P = 0.008$, Saline vs GBR; $F_{(3, 28)} = 9.93$, $P < 0.001$, among ages, two-way repeated-measures ANOVA.

gradual changes with age in the excitability of SNc DA neurons, release of dopamine from DA terminals, and voluntary movement and coordination. From the concordance and correlations between the age-dependency of these changes (Fig. 9 and Table 1), we postulate that age-related alterations in the function of SNc DA neurons and dopamine release may be associated with age-related changes in locomotion and coordination, respectively.

Although our electrophysiological data show that the overall spontaneous firing rate and maximal stimulated firing rate were higher in vSNc DA neurons than in dSNc DA neurons, dSNc and vSNc DA neurons shared several similar features. First, they had a similar proportion of neurons with an irregular firing pattern, and this did not change with age. Second, a large proportion of neurons in both the dSNc and vSNc showed adaptation upon depolarizing stimulation in young, middle-aged, and old animals. Above all, both dSNc and vSNc DA neurons exhibited a reverse V-shaped age-dependent alteration in spontaneous firing rate. Although vSNc DA neurons are more vulnerable to degeneration than dSNc DA neurons in aged subjects [4, 22], these two groups of DA neurons exhibit similar age-dependent alterations in spontaneous firing and survival. It is noteworthy that dSNc and vSNc DA neurons differed in the age-related modification of their responses to depolarizing stimulation. The responses in dSNc DA neurons were the strongest in the 12-month-old group, followed by the 24-month-old group and then the 6-month-old group; however, responses in vSNc DA neurons increased from the 6- to the 12- to the 24-month-old group. Our data provide an overview of the similarities and differences in firing rates and firing patterns between dSNc and vSNc DA neurons across ages.

I_h is an electrophysiological signature of midbrain DA neurons, although I_h amplitude is diverse among individual neurons

[40, 50–52]. In aging rats, we observed that the I_h amplitude in dSNc DA neurons exhibited a 50%–70% reduction at 12 months, relative to the amplitude at 6 months, with a partial recovery at 24 months; however, the I_h amplitude in vSNc DA neurons showed a downward trend with age. I_h has been demonstrated to positively affect pace-maker firing in DA neurons [40, 44]. However, we observed that accompanying the reduction in I_h, the firing rate was higher in DA neurons from 12-month-old rats than 6- or 24-month-old rats. This suggests that SNc DA neurons may be subjected to enhanced excitatory drive during aging, and the reduction in I_h may be a compensatory or protective mechanism. Further investigations are required to elucidate the cellular and molecular mechanisms underlying this contradiction.

Using a newly developed dopamine sensor [30], we observed that the level of dopamine released from striatal terminals in response to a single electrical stimulus reduced with age. These data are consistent with previous studies showing that in aged subjects, the striatum has lower DA content and striatal DA terminals release less dopamine [4, 10, 26]. We revealed that not only the number but also the release probability of DA terminals began to reduce as early as 12 months of age. We also provided data showing that, in old mice, responses evoked by five electrical pulses at 1 Hz displayed more discernable peaks than the responses in young adult mice, and the response amplitudes decayed less robustly in older mice than in young adult mice. According to the known relationship between neurotransmitter release probability and the available pool of active neurotransmitter vesicles, our data suggest that dopamine release probability is more severely damaged in old age than in middle age. It is reasonable that the reduced levels of dopamine release can be compensated for by increasing stimulation frequency (≥ 5 Hz) in

Aging nigrostriatal dopaminergic system and motor deficits
JP Fan et al.

873
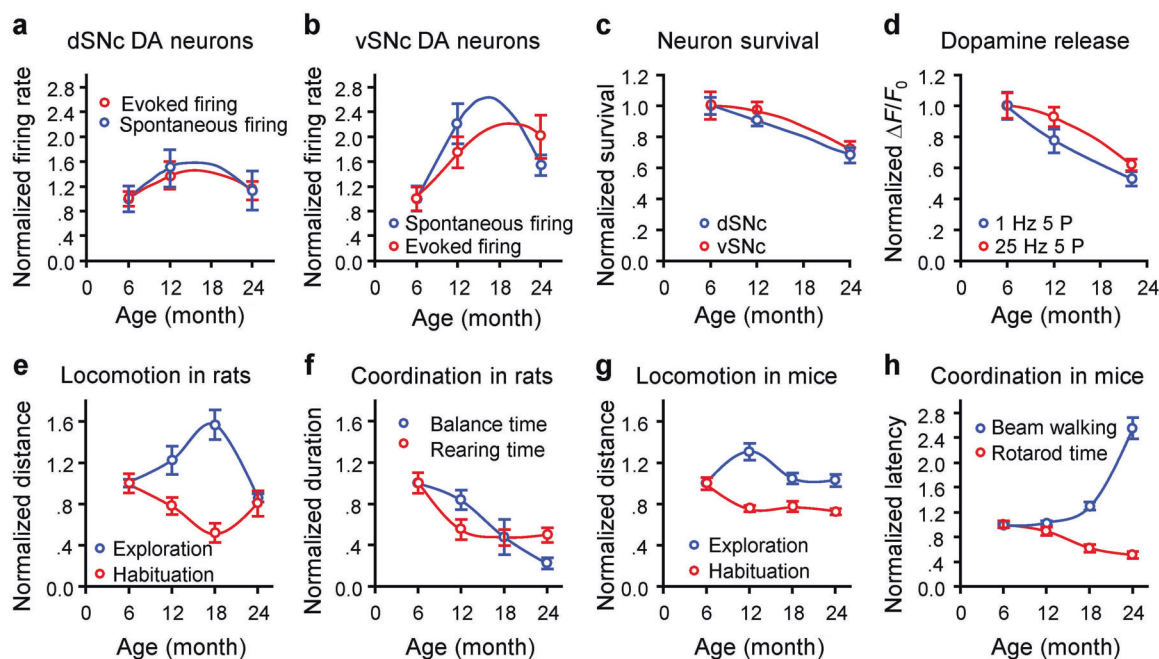
Fig. 9 **Summary of age-dependent alterations in the nigrostriatal dopaminergic system and motor functions. a** Spontaneous firing rate and maximal evoked firing rate in rat dSNc DA neurons were normalized to the averages in neurons from 6-month-old rats. **b** Spontaneous firing rate and maximal evoked firing rate in rat vSNc DA neurons were normalized to the averages in neurons from 6-month-old rats. **c** The numbers of dSNc and vSNc DA neurons in rats were normalized to those observed in 6-month-old rats. **d** Dopamine release ($\Delta F/F_0$) evoked by electrical stimulation (5 pulses at 1 Hz and 25 Hz) was normalized to that observed in 6-month-old mice. **e** Moving distances in the first 5 min in an open field arena and the ratio of last/first 5 min distances in rats were normalized to the averages in 6-month-old rats. **f** Duration on the balancing beam and cylinder rearing time in rats were normalized to the averages in 6-month-old rats. **g** Moving distance in the first 5 min in an open field arena and the ratio of the last 5 min distance to the first 5 min distance in mice were normalized to the averages in 6-month-old mice. **h** Latencies to traverse a walking beam and to fall from the rotarod in mice were normalized to the averages in 6-month-old mice.

middle-aged mice, but not in old mice. In fact, the loss of SNc DA neurons and striatal DA terminals could critically contribute to the severe impairment in dopamine release observed in old mice.

With respect to locomotor behaviors, we observed that, in comparison with the young adult and old groups, middle-aged rats and early middle-aged mice showed more vigorous movement immediately after being placed in an open field arena, followed by habituation. This locomotor hyperactivity concurred with the enhanced excitability of dSNc and vSNc DA neurons at this age. The concurrence of these two age-related changes complies with the notion that SNc DA neurons play a critical role in basic movement through tonic firing [20, 53, 54] and drive invigorated movement through burst firing [20]. Noteworthily, our data show that striatal dopamine release was compromised in middle-aged mice. This appears contradictory with the notion that increased, not decreased, dopamine release enhances movement [55, 56]. We argue that the reduced dopamine release could be overcome by enhanced excitability in SNc DA neurons in middle-aged mice, which is supported by our data showing that repetitive stimuli (>5 Hz) increased dopamine release in 12-month-old mice. This could lead to enhanced movement. Indeed, elevating dopamine levels with a dopamine transporter inhibitor enhanced locomotion in all age groups. It should be mentioned that some midbrain DA neurons co-release dopamine and glutamate in the striatum [57, 58]. Further investigations are warranted to address whether these neurons contribute to the association between hyperexcitability of SNc DA neurons and hyper-locomotion in middle-aged mice.

In a putative parkinsonian transgenic mouse model, Lam et al. found that the mice develop hyperactivity both in the nigrostriatal DA pathway and in locomotion, before the development of parkinsonian neurochemical features (loss of DA neurons) and

motor deficits (akinesia, bradykinesia, etc) [59]. According to this study, the enhanced excitability of SNc DA neurons and the locomotor hyperactivity we observed in 12- and 18-month-old rats and 12-month-old mice may be pre-aged changes, and the recovery of these functional parameters at the age of 24 months may hint at the forthcoming declines in both neuronal activity and locomotion in rats and mice at more advanced ages.

In addition to gross locomotor behavior, we observed that limb coordination deteriorated with aging. Unlike age-dependent changes in the functional properties of SNc DA neurons and gross locomotion, the deterioration of coordination became significant during late middle age and worsened thereafter. These data suggest that the contribution of the observed malfunction in SNc DA neurons to the coordination deficits in the aging process may be limited. On the contrary, age-related deterioration in coordination may be associated with compromised dopamine levels, which are determined by the number of DA neurons and terminals and dopamine release probability. In early middle-aged mice, dopamine release was lower than in younger mice, but these mice did not show deficits in coordination. We argue that in this situation, the decline in dopamine release may not be severe enough to affect coordination because it can be compensated for by enhanced SNc DA neuron firing. But by late middle age and old age, dopamine release declined severely and SNc DA neuron activity returned to normal levels, resulting in lower dopamine levels. The association between reduced release of striatal dopamine and deficits in coordination is further supported by the fact that elevating dopamine levels with a dopamine transporter inhibitor improved coordination in late middle-aged and old mice.

In this study, we recruited aging cohorts of rats and mice aged 6, 12, 18, and 24 months old. Besides the findings that locomotion

Aging nigrostriatal dopaminergic system and motor deficits
JP Fan et al.

874

Table 1. Relationship between TH-positive neurons and terminals and motor function.

	Motor function			
	Distance	Latency in beam walking	Latency in rotarod	Maximal speed in rotarod
Number of DA neurons				
In dSNc ($n = 21$)	0.66 (0.002)**	−0.77 (0.0001)**	0.71 (0.0003)**	0.71 (0.0003)**
In vSNc ($n = 21$)	0.57 (0.008)**	−0.55 (0.01)**	0.39 (0.09)	0.38 (0.10)
TH density ($n = 12$)				
In dorsal striatum	0.35 (0.25)	−0.70 (0.012)*	0.50 (0.09)	0.50 (0.09)

For DA neurons: 6-month, $n = 6$; 12-month, $n = 5$; 18-month, $n = 5$; 24-month, $n = 5$. For striatal TH density: $n = 3$ in 6-, 12-, 18-, and 24-month-old mice. Data were presented as Spearman Rank Order correlation coefficients (P value) between parameters of the nigrostriatal DA system and those quantifying motor function. "n" is the number of mice examined.
*$P < 0.05$;
**$P < 0.01$.

exhibits reverse V-shaped changes with age and coordination deteriorates with age in both rats and mice, we observed some species differences in age-related changes in motor behaviors. First, the distance moved in the first 5 min in the open field arena increased in 12- and 18-month-old rats relative to rats in other age groups, whereas it increased in 12-month-old mice and recovered in 18- and 24-month-old mice. Second, the ratio of distance moved in the last 5 min versus the first 5 min in the open field arena was reduced at 18 months in rats, but at 12 months and later in mice. Third, deterioration in coordination occurred at 12 months in rats but at 18 months in mice. These data suggest that rats and mice age in a similar pattern but at different speeds for locomotion and coordination. Therefore, we postulate that SNc DA neurons and striatal DA terminals in rats and mice may also age in a similar pattern but at different paces. Further investigation is warranted to confirm this possibility.

To summarize, we observed similarities and differences between the activity of dSNc and vSNc DA neurons across ages; the concurrence of age-related modifications in the activity of dSNc and vSNc DA neurons, striatal dopamine release, locomotion, and coordination; and improvements in both locomotion and coordination in middle-aged and old mice with pharmacological elevation of dopamine levels. This study reveals potential associations between SNc DA neuronal activity and locomotion, and between striatal dopamine release and coordination. Our results suggest that different components of the nigrostriatal DA system could be potential intervention targets for different motor phenotypes in aged subjects.

AUTHOR CONTRIBUTIONS
VG and CX designed the experiments. JPF, CX, and CZ performed electrophysiological recordings and imaging, and analyzed the data. JPF, CX, HZG, YWJ, JBT, and TJ acquired and analyzed the behavioral data. CX, CZ, VG, JBT, and AAL wrote the manuscript. All authors read and approved the final version of the manuscript. VG, CX, and CZ supervised the study.

ADDITIONAL INFORMATION
Conflict of interest: The authors declare no competing interests.

REFERENCES
1. Krampe RT. Aging, expertise and fine motor movement. Neurosci Biobehav Rev. 2002;26:769–76.
2. Serrien DJ, Swinnen SP, Stelmach GE. Age-related deterioration of coordinated interlimb behavior. J Gerontol B Psychol Sci Soc Sci. 2000;55:P295–303.
3. Newman RP, LeWitt PA, Jaffe M, Calne DB, Larsen TA. Motor function in the normal aging population: treatment with levodopa. Neurology. 1985;35:571–3.
4. Collier TJ, Kanaan NM, Kordower JH. Ageing as a primary risk factor for Parkinson's disease: evidence from studies of non-human primates. Nat Rev Neurosci. 2011;12:359–66.
5. Levin O, Fujiyama H, Boisgontier MP, Swinnen SP, Summiers JJ. Aging and motor inhibition: a converging perspective provided by brain stimulation and imaging approaches. Neurosci Biobehav Rev. 2014;43:100–17.
6. Wilkinson DJ, Piasecki M, Atherton PJ. The age-related loss of skeletal muscle mass and function: measurement and physiology of muscle fibre atrophy and muscle fibre loss in humans. Ageing Res Rev. 2018;47:123–32.
7. Crupi AN, Nunnelee JS, Taylor DJ, Thomas A, Vit JP, Riera CE, et al. Oxidative muscles have better mitochondrial homeostasis than glycolytic muscles throughout life and maintain mitochondrial function during aging. Aging. 2018;10:3327–52.
8. Nielsen JL. Ageing of human skeletal muscle–myofibre reinnervation as a protective determinant of age-related loss of physical function. J Physiol. 2020;598:29–31.
9. Allen E, Carlson KM, Zigmond MJ, Cavanaugh JE. L-DOPA reverses motor deficits associated with normal aging in mice. Neurosci Lett. 2011;489:1–4.
10. Cruz-Muros I, Afonso-Oramas D, Abreu P, Barroso-Chinea P, Rodríguez M, González MC, et al. Aging of the rat mesostriatal system: differences between the nigrostriatal and the mesolimbic compartments. Exp Neurol. 2007;204:147–61.
11. Emborg ME, Ma SY, Mufson EJ, Levey AI, Taylor MD, Brown WD, et al. Age-related declines in nigral neuronal function correlate with motor impairments in rhesus monkeys. J Comp Neurol. 1998;401:253–65.
12. Floel A, Vomhof P, Lorenzen A, Roesser N, Breitenstein C, Knecht S. Levodopa improves skilled hand functions in the elderly. Eur J Neurosci. 2008;27:1301–7.
13. Vaillancourt DE, Spraker MB, Prodoehl J, Zhou XJ, Little DM. Effects of aging on the ventral and dorsal substantia nigra using diffusion tensor imaging. Neurobiol Aging. 2012;33:35–42.
14. Parkinson GM, Dayas CV, Smith DW. Age-related gene expression changes in substantia nigra dopamine neurons of the rat. Mech Ageing Dev. 2015;149:41–9.
15. Li J, Xia Z, Sun X, Zhang R, Huang G, Hickling R, et al. Reversal of dopamine neurons and locomotor ability degeneration in aged rats with smilagenin. Neuroscience. 2013;245:90–8.
16. Dudman JT, Gerfen CR. The basal ganglia. In: Paxinos G, editor. The rat nervous system. New York: Academic; 2015. p. 391–439.
17. Paxinos G, Watson C. The rat brain in stereotaxic coordinates. 6th ed. New York: Academic Press; 2007.
18. Mazzoni P, Hristova A, Krakauer JW. Why don't we move faster? Parkinson's disease, movement vigor, and implicit motivation. J Neurosci. 2007;27:7105–16.
19. Panigrahi B, Martin KA, Li Y, Graves AR, Vollmer A, Olson L, et al. Dopamine is required for the neural representation and control of movement vigor. Cell. 2015;162:1418–30.

Aging nigrostriatal dopaminergic system and motor deficits
JP Fan et al.

875

20. da Silva JA, Tecuapetla F, Paixao V, Costa RM. Dopamine neuron activity before action initiation gates and invigorates future movements. Nature. 2018;554:244–8.

21. Xiao C, Cho JR, Zhou C, Treweek JB, Chan K, McKinney SL, et al. Cholinergic mesopontine signals govern locomotion and reward through dissociable midbrain pathways. Neuron. 2016;90:333–47.

22. Collier TJ, Kanaan NM, Kordower JH. Aging and Parkinson's disease: Different sides of the same coin? Mov Disord. 2017;32:983–90.

23. Freeman AS, Kelland MD, Rouillard C, Chiodo LA. Electrophysiological characteristics and pharmacological responsiveness of midbrain dopaminergic neurons of the aged rat. J Pharmacol Exp Ther. 1989;249:790–7.

24. Ishida Y, Kozaki T, Isomura Y, Ito S, Isobe K. Age-dependent changes in dopaminergic neuron firing patterns in substantia nigra pars compacta. J Neural Transm Suppl. 2009;73:129–33.

25. Branch SY, Sharma R, Beckstead MJ. Aging decreases L-type calcium channel currents and pacemaker firing fidelity in substantia nigra dopamine neurons. J Neurosci. 2014;34:9310–8.

26. Stamford JA. Development and ageing of the rat nigrostriatal dopamine system studied with fast cyclic voltammetry. J Neurochem. 1989;52:1582–9.

27. Carter RJ, Morton J, Dunnett SB. Motor coordination and balance in rodents. Curr Protoc Neurosci. 2001; Chapter 8: Unit 8 12.

28. Pierce RC, Kalivas PW. Locomotor behavior. Curr Protoc Neurosci. 2007; Chapter 8: Unit 8 1.

29. Tarantini S, Yabluchanskiy A, Fülöp GA, Kiss T, Perz A, O'connor D, et al. Age-related alterations in gait function in freely moving male C57BL/6 mice: translational relevance of decreased cadence and increased gait variability. J Gerontol A Biol Sci Med Sci. 2019;74:1417–21.

30. Sun F, Zeng J, Jing M, Zhou J, Feng J, Owen SF, et al. A genetically encoded fluorescent sensor enables rapid and specific detection of dopamine in flies, fish, and mice. Cell. 2018;174:481–96. e19-496

31. Xiao C, Miwa JM, Henderson BJ, Wang Y, Deshpande P, McKinney SL, et al. Nicotinic receptor subtype-selective circuit patterns in the subthalamic nucleus. J Neurosci. 2015;35:3734–46.

32. Luan Y, Tang D, Wu H, Gu W, Wu Y, Cao JL, et al. Reversal of hyperactive subthalamic circuits differentially mitigates pain hypersensitivity phenotypes in parkinsonian mice. Proc Natl Acad Sci USA. 2020;117:10045–54.

33. Zhou C, Gu W, Wu H, Yan X, Deshpande P, Xiao C, et al. Bidirectional dopamine modulation of excitatory and inhibitory synaptic inputs to subthalamic neuron subsets containing alpha4beta2 or alpha7 nAChRs. Neuropharmacology. 2019;148:220–8.

34. Rodriguez-Oroz MC, Rodriguez M, Guridi J, Mewes K, Chockkman V, Vitek J, et al. The subthalamic nucleus in Parkinson's disease: somatotopic organization and physiological characteristics. Brain. 2001;124:1777–90.

35. Schneider CA, Rasband WS, Eliceiri KW. NIH Image to ImageJ: 25 years of image analysis. Nat Methods. 2012;9:671–5.

36. Noldus LP, Spink AJ, Tegelenbosch RA. EthoVision: a versatile video tracking system for automation of behavioral experiments. Behav Res Methods Instrum Comput. 2001;33:398–414.

37. Clifton GL, Jiang JY, Lyeth BG, Jenkins LW, Hamm RJ, Hayes RL. Marked protection by moderate hypothermia after experimental traumatic brain injury. J Cereb Blood Flow Metab. 1991;11:114–21.

38. Schallert T, Fleming SM, Leasure JL, Tillerson JL, Bland ST. CNS plasticity and assessment of forelimb sensorimotor outcome in unilateral rat models of stroke, cortical ablation, parkinsonism and spinal cord injury. Neuropharmacology. 2000;39:777–87.

39. Dean AG, Sullivan KM, Soe MM. OpenEpi: Open source epidemiologic statistics for public health, version 2.3.1. www.OpenEpi.com (2010).

40. Roeper J. Dissecting the diversity of midbrain dopamine neurons. Trends Neurosci. 2013;36:336–42.

41. Schultz W. Multiple functions of dopamine neurons. F1000 Biol Rep. 2010;2:2.

42. Branch SY, Chen C, Sharma R, Lechleiter JD, Li S, Beckstead MJ. Dopaminergic neurons exhibit an age-dependent decline in electrophysiological parameters in the MitoPark Mouse Model of Parkinson's disease. J Neurosci. 2016;36:4026–37.

43. Kish SJ, Shannak K, Rajput A, Deck JH, Hornykiewicz O. Aging produces a specific pattern of striatal dopamine loss: implications for the etiology of idiopathic Parkinson's disease. J Neurochem. 1992;58:642–8.

44. He C, Chen F, Li B, Hu Z. Neurophysiology of HCN channels: from cellular functions to multiple regulations. Prog Neurobiol. 2014;112:1–23.

45. Floresco SB, West AR, Ash B, Moore H, Grace AA. Afferent modulation of dopamine neuron firing differentially regulates tonic and phasic dopamine transmission. Nat Neurosci. 2003;6:968–73.

46. Yang H, de Jong JW, Tak Y, Peck J, Bateup HS, Lammel S. Nucleus accumbens subnuclei regulate motivated behavior via direct inhibition and disinhibition of VTA dopamine subpopulations. Neuron. 2018;97:434–49. e4-449

47. Zhang Z, Liu Q, Wen P, Zhang J, Rao X, Zhou Z, et al. Activation of the dopaminergic pathway from VTA to the medial olfactory tubercle generates odor-preference and reward. Elife. 2017;6:6.

48. Lopes EF, Roberts BM, Siddorn RE, Clements MA, Cragg SJ. Inhibition of nigrostriatal dopamine release by striatal GABA$_A$ and GABA$_B$ receptors. J Neurosci. 2019;39:1058–65.

49. Zhang H, Sulzer D. Frequency-dependent modulation of dopamine release by nicotine. Nat Neurosci. 2004;7:581–2.

50. Lammel S, Hetzel A, Hackel O, Jones I, Liss B, Roeper J. Unique properties of mesoprefrontal neurons within a dual mesocorticolimbic dopamine system. Neuron. 2008;57:760–73.

51. Margolis EB, Lock H, Hjelmstad GO, Fields HL. The ventral tegmental area revisited: is there an electrophysiological marker for dopaminergic neurons? J Physiol. 2006;577:907–24.

52. Xiao C, Shao XM, Olive MF, Griffin WC 3rd, Li KY, Krnjević K, et al. Ethanol facilitates glutamatergic transmission to dopamine neurons in the ventral tegmental area. Neuropsychopharmacology. 2009;34:307–18.

53. Dragicevic E, Schiemann J, Liss B. Dopamine midbrain neurons in health and Parkinson's disease: emerging roles of voltage-gated calcium channels and ATP-sensitive potassium channels. Neuroscience. 2015;284:798–814.

54. Surmeier DJ, Schumacker PT. Calcium, bioenergetics, and neuronal vulnerability in Parkinson's disease. J Biol Chem. 2013;288:10736–41.

55. Grillner S, Robertson B. The basal ganglia over 500 million years. Curr Biol. 2016;26:R1088–R100.

56. Palmiter RD. Dopamine signaling in the dorsal striatum is essential for motivated behaviors: lessons from dopamine-deficient mice. Ann N. Y Acad Sci. 2008; 1129:35–46.

57. von Twickel A, Kowatschew D, Saltürk M, Schauer M, Robertson B, Korsching S, et al. Individual dopaminergic neurons of Lamprey SNc/VTA project to both the striatum and optic tectum but restrict co-release of glutamate to striatum only. Curr Biol. 2019;29:677–85. e6-685

58. Morales M, Root DH. Glutamate neurons within the midbrain dopamine regions. Neuroscience. 2014;282:60–8.

59. Lam HA, Wu N, Cely I, Kelly RL, Hean S, Richter F, et al. Elevated tonic extracellular dopamine concentration and altered dopamine modulation of synaptic activity precede dopamine loss in the striatum of mice overexpressing human alpha-synuclein. J Neurosci Res. 2011;89:1091–102.